Available online at www.sciencedirect.com
ScienceDirect
International Journal of Thermal Sciences 46 (2007) 139–148
International Journal of Thermal Sciences
www.elsevier.com/locate/ijts

Experimental study on forced convective heat transfer characteristics in quartz microtube

Zhi-Gang Liu [a,*], Shi-Qiang Liang [b], Masahiro Takei [c]

[a] *Energy Research Institute of Shandong Academy of Sciences, Jinan 250014, China*
[b] *Institute of Engineering Thermophysics, Chinese Academy of Sciences, Beijing 100080, China*
[c] *Department of Mechanical Engineering, Nihon University, Tokyo 101-8308, Japan*

Received 27 October 2005; received in revised form 22 March 2006; accepted 29 March 2006

Available online 5 June 2006

Abstract

Experiments were carried out to investigate forced convective heat transfer of deionized water flowing through quartz microtubes with inner diameter of 242, 315 and 520 μm. The microtube was heated by directly electrifying a brass wire that was coiled evenly up around the microtube to keep a constant heat flux, or heated by steam to keep a constant temperature. As Reynolds number varied in the range from 100 up to 5000–7000 in the experiments, the corresponding Nusselt numbers were also measured. The experimental results were compared with those of the classical correlations for convective heat transfer in a laminar, transitional or turbulent regime for conventional tubes, and a difference was found. The comparisons indicated that the Nusselt number tends to be agreement with those of the classical laminar correlations at a lower Reynolds number, and increased sharply with the increasing of Reynolds number. If Reynolds number was larger than 1500, 1600 and 1900 for microtubes with inner diameter of 242, 315 and 520 μm, respectively, the corresponding Nusselt number was higher than the predictions by the classical transitional correlations. When Nusselt number reached the value from the classical turbulent correlations, Reynolds number was approximately equal to 4000, 4500 and 5500, respectively, for these types of microtubes.

Keywords: Microtube; Forced convective heat transfer; Constant heat flux; Constant temperature; Reynolds number; Nusselt number

1. Introduction

Owing to the microfabrication technology development of integrated circuits, smaller tubes can be made and used for increasing the compactness of heat exchangers. These micro heat exchangers are able to attain extremely high heat transfer surface area per unit volume, high heat transfer coefficient, and low thermal resistance. This has been motivated by their proposed use in such concrete applications as micro power generation, computer chips and chemical separations processes [1] etc. Up to now, a number of investigators have performed many researches, especially on experimental studies.

In fact, the micro-channel heat sink cooling concept was first introduced by Tuckerman and Pease in the early 1980s [2]. Mala and Li [3] investigated experimentally the flow characteristics of water in microtubes with diameters ranging from 50 to 254 μm. For tubes with small diameters the experimental results on friction factor show a significant departure from the conventional theory, while for tubes with large diameters the experimental results are in good agreement with the classical theory. The authors explained this unusual phenomenon by introducing the roughness viscosity model, which takes into account increase of the momentum transfer in the boundary layer near the wall due to the presence of roughness. Adams et al. [4] performed an experimental investigation of heat transfer characteristics of water in microtubes ranging from 760 to 1090 μm. They found that the experimental Nusselt number were higher than those predicted by conventional heat transfer correlations. The authors observed that the extent of the heat transfer enhancement (defined as deviation from the conventional theory) increased as the channels diameter decreased and Reynolds number increased. Lelea et al. [5] analyzed experimentally the developing microchannels heat transfer and fluid flow on tubes

* Corresponding author.
E-mail address: zgliu9322@yahoo.com.cn (Z.-G. Liu).

1290-0729/$ – see front matter
doi:10.1016/j.ijthermalsci.2006.03.008

Nomenclature

C_p	specific heat at constant pressure	$J\,kg^{-1}\,K^{-1}$
d	inner diameter of microtube	m
D	outer diameter of microtube	m
F	area of the inner wall of microtube	m^2
L	length of microtube	m
k	fluid thermal conductivity	$W\,m^{-2}\,K^{-1}$
ΔT	temperature difference between the inner wall and the outer wall of microtube	K
u	fluid velocity	$m\,s^{-1}$
x	distance	m

Greek symbols

μ	dynamic viscosity	$kg\,m^{-1}\,s^{-1}$
Nu	Nusselt number	
Pr	Prandtl number	
q	heat flux	$W\,m^{-2}$
Q_t	heat	W
Q_V	volumetric flow rate	$m^3\,s^{-1}$
R	resistance	Ω
Re	Reynolds number	
Δt	temperature difference between the inlet and the outlet of microtube	
T	temperature	K
T_c	temperature coefficient	K
ρ	density	$kg\,m^{-3}$
ε	uncertainty	μm
η	kinematical viscosity	$m^2\,s^{-1}$

Subscripts

av	average
f	fluid
in	inner
m	mean
0	surroundings
1	inlet of test section
2	outlet of test section

of $D_i = 0.1$, 0.3 and 0.5 mm, having water as a working fluid. The experimental result does not provide any new aspect, but this is meaningful considering the large scattering in the existing results. Lee et al. [6] investigated the heat transfer in microchannels of different sizes ($D_i = 318$–903 μm) over a range of flow rates. The experimental results that the heat transfer coefficient increased with decreasing channel size at a given flow rate and numerical results were found to be in good agreement with the experimental data, suggesting that such approaches, when coupled with carefully matched entrance and boundary conditions, can be employed with confidence for predicting heat transfer behavior in microchannels in the dimensional range considered here. Celata et al. [7] investigated experimentally the forced-convection heat transfer of refrigerant R114 flowing through microtube with diameter of 0.130 mm. Experimental results show that heat transfer correlations in laminar and turbulent regimes developed for conventional tubes are not adequate for calculation of heat transfer coefficient in microtubes.

In the above cited literature, there is considerable disagreement about the effects of microscale on the heat transfer. Some studies showed [2,3,5] that the Nusselt number for microscale heat transfer is higher than those traditional correlations for microscale. Some researchers [8] attributed this enhancement to thinning of the boundary layer in the narrow channels while others [9] considered it was resulted from the size effects of microscale, such as the effect of roughness, the effect of surface geometry, the effect of surface electrostatic charges and the effect of axial heat conduction in the wall of microchannel or microtube etc. Recently, the influence of the axial heat conduction along the wall on the convective heat transfer has been much studied [10,11]. Many researchers have directed great efforts to investigate the influence of the axial heat conduction along the wall on the convective heat transfer. Gamrat et al. [10] numerically analysed the three-dimensional flow and associated heat transfer in a rectangular microchannel heat sink. The numerical simulation considered the coupling between convection in microchannels and conduction in the walls and in the complete solid material. The numerical simulations show that there is no size effect on heat transfer when the channels spacing is reduced from 1 mm down to 0.1 mm. As a result, the strong reduction in the Nusselt number observed in experiments cannot be explained by conduction effects due to the complex geometry, like axial conduction in the walls or lack of two-dimensionality of the heat flux distribution. Further investigations are planned both from the numerical and experimental points of view in order to reduce the gap between the results of the two approaches. However, Maranzana et al. [11] proposed the two analytical models of heat transfer in channel flow between parallel plates and allow the application of an inverse method in order to estimate convective heat transfer coefficients. The authors thought that the axial conduction in walls of mini-micro-devices has to be considered because the effect of the axial conduction along the mini-micro scale wall can lead to very large bias in the experimental estimation of heat transfer coefficients, especially for small Reynolds numbers unless the M (a new non-dimensional number) gets lower than 10^{-2}.

Further systematic studies are required to generate sufficient physical knowledge of the mechanisms responsible for the variation of the heat transfer in microtubes. So more experimental investigations about heat transfer in microtubes are conducted in this paper based on mentioned above.

It is well known that no conventional method, e.g. thermocouple, can obtain the average temperature of the wall of microtube, which is very necessary for obtaining Nusselt number in microtube. In this paper, we managed to obtain the average temperature of the outer wall of microtube by introducing two approaches according to heating mode. In the mode of constant heat flux heating, the average temperature is associated with the resistance change of the heating brass wire, and in the

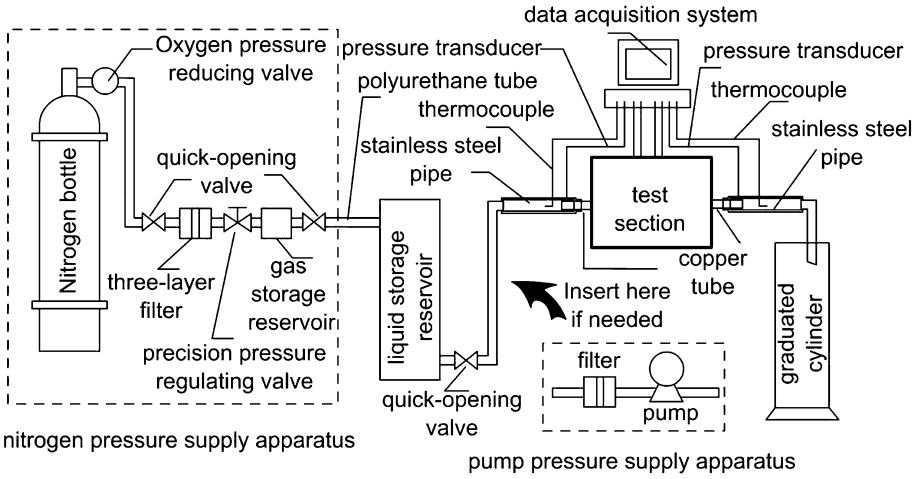

Fig. 1. Schematic illustration of the experimental loop.

mode of constant temperature heating, the average temperature is assumed to be the constant condensation temperature of the heating saturated steam.

The objective of the present study is to investigate the single-phase heat transfer behavior of deionized water in microtubes with inner diameters of 242 μm, 315 μm and 520 μm, respectively. As the Reynolds number varies from 100 up to 5000–7000 in the experiment and the Nusselt number is obtained by using different heating method, that is, the constant heat flux heating and the constant temperature heating. The influence of heating method, hydraulic diameter and flow state on the characteristics of convective heat transfer in microtube will be obtained. Therefore, more details about the forced convective heat transfer in microtubes can be found out, and it is very helpful to understand better the behavior of heat transfer characteristics in such microtubes.

2. Experimental setup and procedure

2.1. Experimental setup

The test rig was schematically illustrated in Fig. 1.

As shown, two apparatus were used to supply pressure, one of which is sourced from a nitrogen bottle of 12 MPa and works at lower pressure than 1.6 MPa, and the other comprises a reciprocating plunger gauge pump (JLB-2B) that is able to supply higher pressure up to 10 MPa and wider flow rate ranged up to 4500 ml h^{-1}. The nitrogen pressure supply system was comprised of a gas storage reservoir, a precision pressure-regulating valve, a three-layer filter, a quick-opening valve and the nitrogen bottle. The gas storage reservoir served as a buffer to avoid fluctuation, the pressure-regulating valve can precisely regulate pressure, and the filter can get rid of particle impurities. The liquid storage reservoir contains the working fluid. The nitrogen bottle, filter and liquid storage reservoir were linked by blow-off proof polyurethane hose, which can resist 2 MPa pressure at most. At each copper tube end of the test section, a stainless steel pipe of 2 cm long or so was plugged into the polyurethane hose and was agglutinated onto the copper tube, and inner diameter of the stainless steel is 2 mm wide. Here, inside each

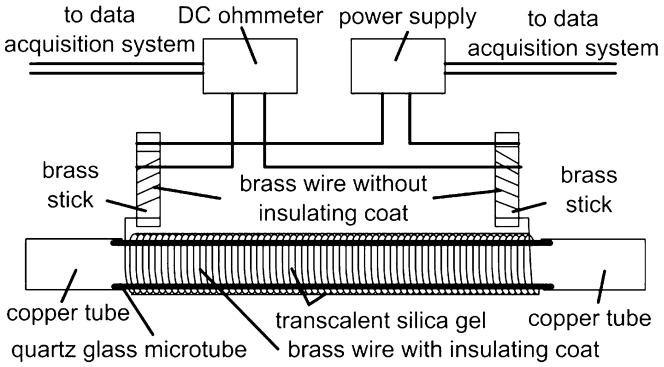

Fig. 2. The test section of constant heat flux heating.

polyurethane hose, that is to say, outside each stainless steel pipes, a K-thermocouple was embedded to measure the inlet and outlet temperature of the fluid flowing through the test section. All the joints were sealed up with rigid seal. A precision graduated cylinder was used to read the flux, when the inlet and outlet temperatures remain constant with flow rate, the weight of fluid flowing out of the test section will be given by reading of the graduated cylinder. Other than the flux, all data can be read from the data acquisition system. When the pressure sources from the pump, a filter and the pump should be inserted between the liquid storage reservoir and the test section, and the pore size of the membrane of the filter is 1 μm around.

2.2. Test section

The experimental loop involved two kinds of test section, that of approximately constant heat flux heating and that of constant temperature heating, and the first one is illustrated in Fig. 2.

This test section shown in Fig. 2 is an approximately constant heat flux heating (because both fluid and microtube wall temperatures are increased along the flow direction, leading to the increased temperature of the heating wire that is wrapped on the outer wall surface of the microtube. The electric resistance and the heating power are strongly varied along the flow direction). A thin brass wire, with the diameter of 80 μm, is uni-

formly coiled around the quartz microtube by a machine, at the same time, transcalent silica gel is wiped over the brass wire. The silica gel will reduce the heat transfer resistance between the brass wire and the wall of microtube; in addition, it will cement the wire and the microtube. As it was shown in Fig. 2, both ends of the wire were coiled around brass sticks, and their insulating coat had been wiped off. The heating power supply (DH1716A) can supply low voltage but large current. The DC ohmmeter (ZRC-V) can detect a minimum resistance of 1 μΩ, and the measuring error is not greater than 0.5%. In the case of nitrogen pressure supply system, the quartz microtube with the brass wire coiled around and the copper pipe were connected up by high strength 914-glue (can resist high temperature of 140 °C). While in case of pump pressure supply system, they were connected up by a metal turnbuckle and the 914-glue. Because the insulating coat of the brass wire cannot resist higher temperature than 120 °C, so temperature of the wire must be detected by the rapid DC ohmmeter.

The brass wire provider had offered a calculating model for averaged temperature, T_{av} as a function of electric resistance of the brass wire and the tested temperature:

$$T_{av} = \frac{R_h}{R_0}(T_c + T_0) - T_c \tag{1}$$

where, R_0 is called as cold-state resistance at environmental temperature T_0, Ω; R_h is known as hot-state resistance after heating, Ω; T_c is the temperature coefficient, varying with different materials, in this experiment, it is 235 °C.

The room temperature is measured by a thermocouple with resolution of 0.1 °C and the resistance of the wire is also measured at the same time in advance. When the inlet temperature and outlet temperature do not vary with flow rate, the hot-state resistance is read rapidly, and the average temperature T_{av} can be calculated by Eq. (1).

Because of the silica gel, the brass wire contacts closely with wall of the microtube, so the averaged temperature approximates temperature of the wall surface very well. Whereas the difference of temperature, ΔT of the inner wall and the outer one can be expressed as:

$$\Delta T = \frac{Q_t \ln(\frac{D}{d})}{2\pi kL} \tag{2}$$

Q_t is heat flux:

$$Q_t = C_p \rho Q_V \Delta t \tag{3}$$

There is a thermal resistance resulted from the contacting thermal resistance between the brass wire and outer wall of microtube and the temperature ΔT_1, resulted from the thermal resistance, can be expressed as:

$$\Delta T_1 = \frac{Q_t \ln(2\Delta x_1 + D)}{2\pi k_s L} \tag{4}$$

where, Δx_1 is the average distance from transcalent silica gel between the brass wires to outer wall of microtube, m. It can be obtained by integral and its value is approximately equal to $(40–5\pi)$ μm in present experiment.

In fact, ΔT_1 is very small due to extremely small dimensions and is approximately equal to 0.05–0.3 °C when the heating quantity is not large. However, ΔT_1 will apparently increase with the increase of heating flux density and the maximal value may reach 1 °C.

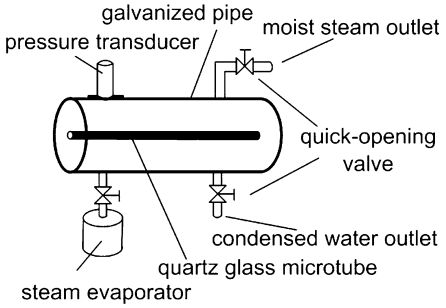

Fig. 3. The test section of constant temperature heating.

So the actual temperature of the inner wall of the microtube, T_{in}, can be expressed as:

$$T_{in} = T_{av} - \Delta T - \Delta T_1 \tag{5}$$

Further, there are some other uncertainties, such as the cold or hot state resistance measurement, the thickness of the insulating coat measurement and the distributing uniformity of transcalent silica gel, etc., which result in about 0.3 °C temperature measuring errors according to systematical analysis.

The second test section, illustrated in Fig. 3, is of constant temperature heating.

As same as that of constant heat flux heating, the test section was connected to the test loop by 914-glue or a metal turnbuckle and 914-glue. The steam evaporator (DZ-300) can generate steam up to 24 ml per minute. The steam flows into the galvanized pipe and heats the quartz microtube. In the experiment, the moist steam outlet quick-opening valve should be opened firstly, once steam spurts out of the outlet, close the outlet valve. Adjusting the evaporator to a proper heating power, the condensed water outlet valve is slightly opened, so that the whole quartz microtube is well immersed in saturated steam. The condensation heat transfer coefficient of outer wall should be confirmed to be larger than the convective heat transfer coefficient in microtube and thus the constant wall temperature can be kept. Based on this reason, the experimental Nusselt number at higher Reynolds number (for example, $Re > 5000$ for microtube with inner 242 μm) cannot be exactly obtained. A pressure transducer on the galvanized pipe was used to monitor the pressure inside the pipe, so that temperature of the saturated steam, also temperature of the quartz microtube's wall surface T_m, can be obtained directly. And the inner surface temperature T_{in} can be calculated by:

$$T_{in} = T_m - \Delta T \tag{6}$$

Here, ΔT can be obtained from Eq. (2).

2.3. Geometric size of the microtube

This experiment involved three quartz glass microtubes. Length of each microtube, L, was measured by a vernier caliper, and its diameter, D, was measured by a micrometer.

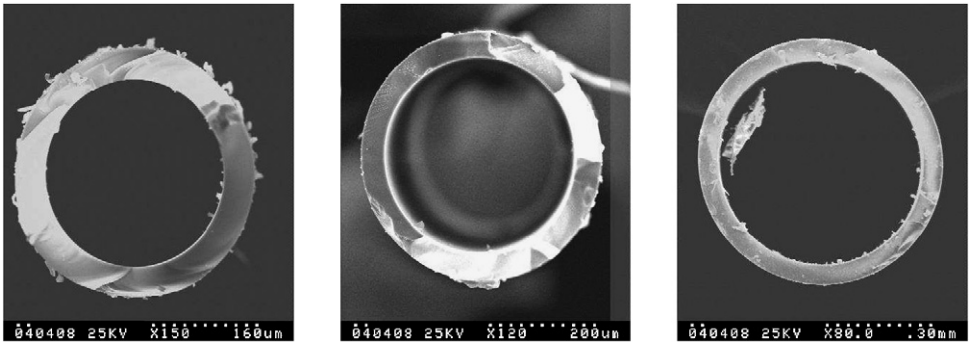

Fig. 4. SEM images of the cross-section of quartz glass microtubes with inner diameters of 242 μm, 315 μm and 520 μm.

Table 1
Geometrical size of each microtube and the measuring error

L [mm]	ε_1 [μm]	D [μm]	ε_2 [μm]	d [μm]	ε_3 [μm]
148.27	±20	446	±5	242	±1.21
148.44	±20	556	±5	315	±1.58
148.61	±20	812	±5	520	±2.60

Table 2
Experimental uncertainties (%)

Variable	$Re < 1000$	$1000 < Re < 2500$	$Re > 2500$
Δt	±0.2 °C	±0.2 °C	±0.2 °C
ρ	0.6	0.5	0.2
μ	0.7	0.6	0.4
u	2.3	1	0.5
Re	5.9	5.7	5.6
Nu	16	9.8	7.8

Recurring to SEM image, inner diameter, d, was obtained, as shown in Fig. 4.

The employed electron microscope (S-570) has a high resolving power of 0.1 μm. So the measuring error of the inner diameter will be less than 0.5%, but the unsymmetricalness of the inner diameter along axial flow will lead to an inherent measuring error of 1.33% around, so that the maximum measuring error of flux due to the unsymmetricalness will not exceed 5.0% [7].

The geometrical size of each microtube of three was listed in Table 1.

2.4. Experiment uncertainties

As mentioned above, the volumetric flow rate was measured using a graduated cylinder. All other data can be acquired from the data acquisition system. All data must be measured in steady state. If only the pressure and the temperature kept unvarying, stable state had come. The experiment uncertainties of all data are listed below in Table 2, and the error analysis method comes from reference literature [13].

3. Result and discussion

The experimental setup allows experimental data to be obtained for single-phase forced-convective heat transfer in microtubes. In constant heat flux heating mode, it was the electrified brass wire that heated the outer wall of the microtube, and in the constant temperature mode, it was heated by steam. In the former heating mode, the wall heat flux of the microtube is assumed constant, and the temperature is assumed constant in the latter heating mode. Though thickness of the wall is very thin, the difference in temperature of the outer wall and the inner wall is not negligible due to the tremendous heat flux and the low thermal conductivity of quartz. The exact inner wall temperature can be obtained by Eqs. (1)–(6). The flow rate and the temperature of the inlet and the outlet streams can also be measured. The Nusselt number, Nu_f, therefore, can be expressed by Eq. (7):

$$Nu_f = \frac{C_p \rho Q_V d(t_2 - t_1)}{k_f F(T_{in} - \frac{t_1+t_2}{2})} \tag{7}$$

Experimental results are compared with the correlations of Shah [14], Hausen [15] and Sieder–Tate [16] for the laminar regime, Hausen [17] and Gnielinski [18] for the transitional regime and Gnielinski [18] and Dittus–Boelter [19] for the turbulent regime.

The Shah correlation at constant heat flux on the surface of microtube:

$$Nu_f = \left(4.364 + 0.0722 Re\, Pr \frac{d}{L}\right)\left(\frac{\mu_f}{\mu_w}\right)^{0.14} \tag{8}$$

Eq. (8) has been confirmed experimentally for the range of conditions: $Re \leqslant 2200$, $Re_f Pr_f \frac{d}{L} \leqslant 33.3$, and if the $Re_f Pr_f \frac{d}{L} \geqslant 33.3$, the Shah correlation is:

$$Nu_f = 1.953\left(Re_f Pr_f \frac{d}{L}\right)^{\frac{1}{3}}\left(\frac{\mu_f}{\mu_w}\right)^{0.14} \tag{9}$$

Similarly, for constant wall temperature, Hausen and Sieder–Tate recommend two correlations of the form:

The Hausen correlation (laminar regime):

$$Nu = 3.66 + \frac{0.19(Re_f Pr_f \frac{d}{L})^{0.8}}{1 + 0.117(Re_f Pr_f \frac{d}{L})^{0.467}} \tag{10}$$

$Re_f < 2200$, $Pr = 0.5$–17000, $\eta_f/\eta_w = 0.044$–9.8, $Re_f Pr_f < 10$.

If $Re_f Pr_f > 10$, the Sieder–Tade correlation is proper:

$$Nu = 1.86\left(Re_f Pr_f \frac{d}{L}\right)^{\frac{1}{3}}\left(\frac{\eta_f}{\eta_w}\right)^{0.14} \tag{11}$$

The Hausen correlation (transitional regime) is:

$$Nu_f = 0.116\left(Re_f^{\frac{2}{3}} - 125\right)Pr_f^{\frac{1}{3}}\left[1 + \left(\frac{d}{L}\right)^{\frac{2}{3}}\right]\left(\frac{\mu_f}{\mu_w}\right)^{0.14} \quad (12)$$

$2200 < Re < 10^4$, $Pr_f > 0.6$.

The Gnielinski correlation for transitional regime and turbulent regime is:

$$Nu = \frac{(\frac{f}{2})(Re_f - 1000)Pr_f}{1 + 12.7(\frac{f}{2})^{\frac{1}{2}}(Pr^{\frac{2}{3}} - 1)} \quad (13)$$

$$f = \frac{1}{[3.64\log(Re) - 3.28]^2}, \quad 3000 < Re < 5 \times 10^6.$$

The Dittus–Boelter correlation for turbulent regime is:

$$Nu_f = 0.023Re_f^{0.8}Pr_f^{0.4} \quad (14)$$

The variations of the experimental Nusselt number with Reynolds number are plotted in Figs. 5–6 for different inner diameters and for different heating modes at $Re < 2500$. Comparisons were also drawn between the experimental data and the correlations of Shah, Hausen and Sieder–Tate.

According to Figs. 5–6, the experimental Nusselt number increase with Reynolds number as expected and the dependence is a straight line at the lower Reynolds number (laminar flow). With the increase of Reynolds number, the experimental Nusselt number quickly increases.

When Reynolds number is larger than 1500, 1600 and 1900 for microtubes with inner diameters of 242 μm, 315 μm and 520 μm, respectively, the all experimental data are larger than the predictions of the Shah, Hausen and Sieder–Tate correlations, which indicate the flow is no longer laminar, but is in a transitional flow regime, even a turbulent flow regime.

Besides, it looks as if the experimental Nusselt numbers are less than the laminar correlations when Reynolds number is low, shown in Figs. 5–6. However, there may be some effects that may influence the experimental results and lead to relative uncertainties in the present study.

It is difficult to measure the local heat flux at the inner wall of the microtube, the definition of the heat transfer coefficient is very important and will strongly influence the results and how the heat transfer varies along the microtube wall. In present work, because to date all of the experimental data utilizes the temperature at the microtube wall and at the inlet and outlet of the microtube, using the data reduction described in Eq. (7) may lead to some uncertainty as may have been the case in Ref. [20]. On the one hand, the temperature rise along the microtube can be very large at very low values of the Reynolds number when the heat flux at the microtube walls is fixed, the thermophysical properties cannot be considered as constant; in other words, the effects related to the variation of the thermophysical properties with temperature are in general strongly coupled with conjugate effects in microtubes for uniform heated microtube, so the bulk liquid temperature is demonstrated to vary in a nonlinear form along the flow direction for low fluid flow rates, but not for high flow rates, as indicated by J. Li et al. [21], which the experimental data will be less than the real value at low Reynolds number by using Eq. (7). It is well known, on the other hand, that in the region of low Reynolds numbers the effects of the conjugated heat transfer in microtubes on the mean value of the Nusselt number are felt because conduction along the microtube walls can become a competitive mechanism of heat transfer with respect to the internal convection, as indicated by Maranzana et al. [11] and Gamrat et al. [8]. Heat transfer by conduction along the walls of microchannels can induce a quite multidimensional pattern of temperature distribution [6,12,21]. These works demonstrated that the experimental evaluation of the convective heat transfer coefficient between the fluid and the walls of a microchannel requires the use of a conduction model for the walls because local direct measurements of temperature and wall heat flux at the interface are very difficult. As evidenced by Maranzana et al. [11], when the effects of conjugate heat transfer are predominant, the temperature of distribution along the microchannel is not linear at all and the wall heat flux becomes not uniform along the microchannel. For this reason, the Nusselt number calculated by using the mean value of the fluid bulk temperature at the inlet and outlet of the microchannel is general underestimated. This is a reason why the experimental values of the mean Nusselt number disagree with the theoretical one for fully developed flow, especially at low Reynolds numbers. This disagreement tends to decrease with the increment of Reynolds number because the effects of the conjugate heat transfer are then limited. The dependence of the Nusselt number with the Reynolds number for low values is thus explained. However, the effect of conjugate heat transfer would not operate in a general way unless some conditions (indicated by Maranzana et al. [11]) were met. In our present work, the effect of conjugate heat transfer may not be predominant only when the Reynolds number is very low.

In addition, the uncertainties result from the measurements may cause further deviation besides the reasons mentioned above. So the experimental Nusselt number may be rough agreement with prediction by the conventional classical correlations at lower Reynolds number unless the Reynolds number is extremely low.

With the Reynolds number further increase ($1000 < Re < 7000$), the experimental Nusselt number are compared with that of the correlations of Hausen and Gnielinski for the transitional regime and Gnielinski and Dittus–Boelter for turbulent regime are shown in Figs. 7–8.

Although the focus of the present work is on laminar state, the experiments extended into the turbulent range as well, to a Reynolds number of 7000. Beyond a range of Reynolds number of approximately 1500–1900, the experimental results show a change in slope, reflecting a transition from laminar flow. As seen in Figs. 7–8, the experimental Nusselt numbers are generally higher in the transitional region than predictions from correlations of Eqs. (12)–(13) when Reynolds number is larger than 1500, 1600 and 1900 for microtubes of inner diameters 242 μm, 315 μm and 520 μm, respectively. Predictions from the Gnielinski and Dittus–Boelter correlations, on the other hand, are seen to lie down the experimental data, possibly because they were proposed for fully turbulent flow when

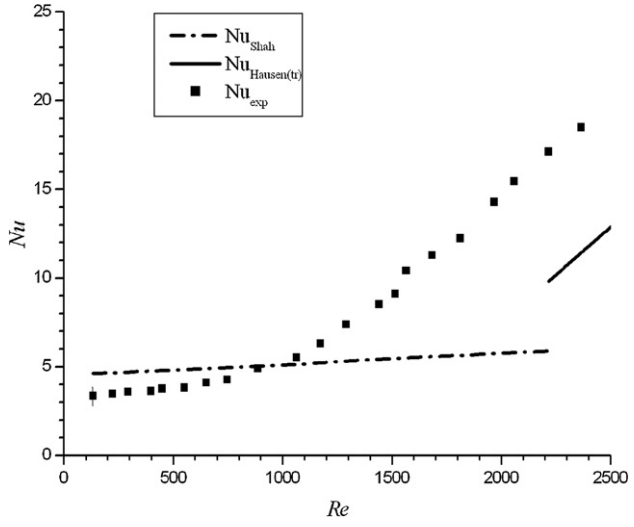

(a)

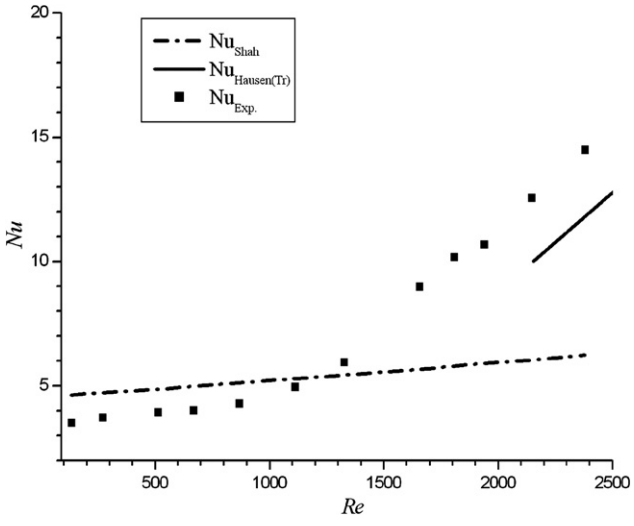

(b)

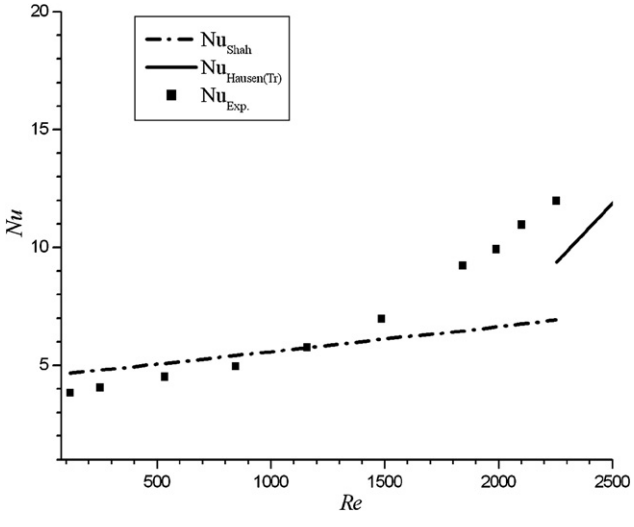

(c)

Fig. 5. Comparison of Nusselt numbers between experimental data and classical correlations ($Re < 2500$) for three microtubes at constant heat flux heating method: (a) $d = 242$ μm and $t_1 = 21.4\,^{\circ}\mathrm{C}$; (b) $d = 315$ μm and $t_1 = 21.8\,^{\circ}\mathrm{C}$; (c) $d = 520$ μm and $t_1 = 21.8\,^{\circ}\mathrm{C}$.

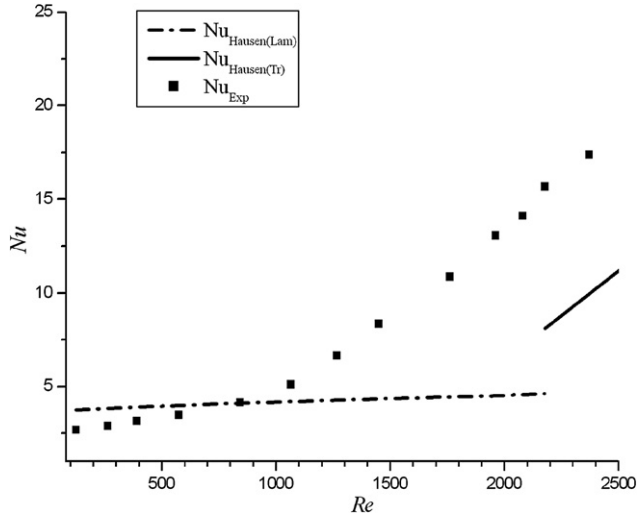

(a)

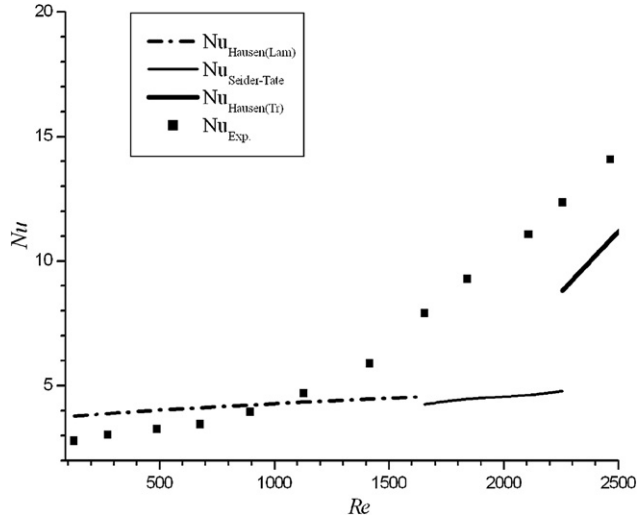

(b)

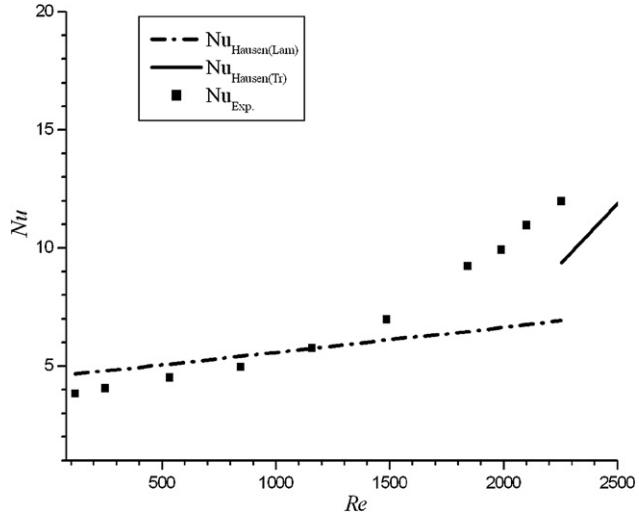

(c)

Fig. 6. Comparison of Nusselt numbers between experimental data and classical correlations ($Re < 2500$) for three microtubes at constant temperature heating method: (a) $d = 242$ μm and $t_1 = 21.4\,^{\circ}\mathrm{C}$; (b) $d = 315$ μm and $t_1 = 21.7\,^{\circ}\mathrm{C}$; (c) $d = 520$ μm and $t_1 = 23.4\,^{\circ}\mathrm{C}$.

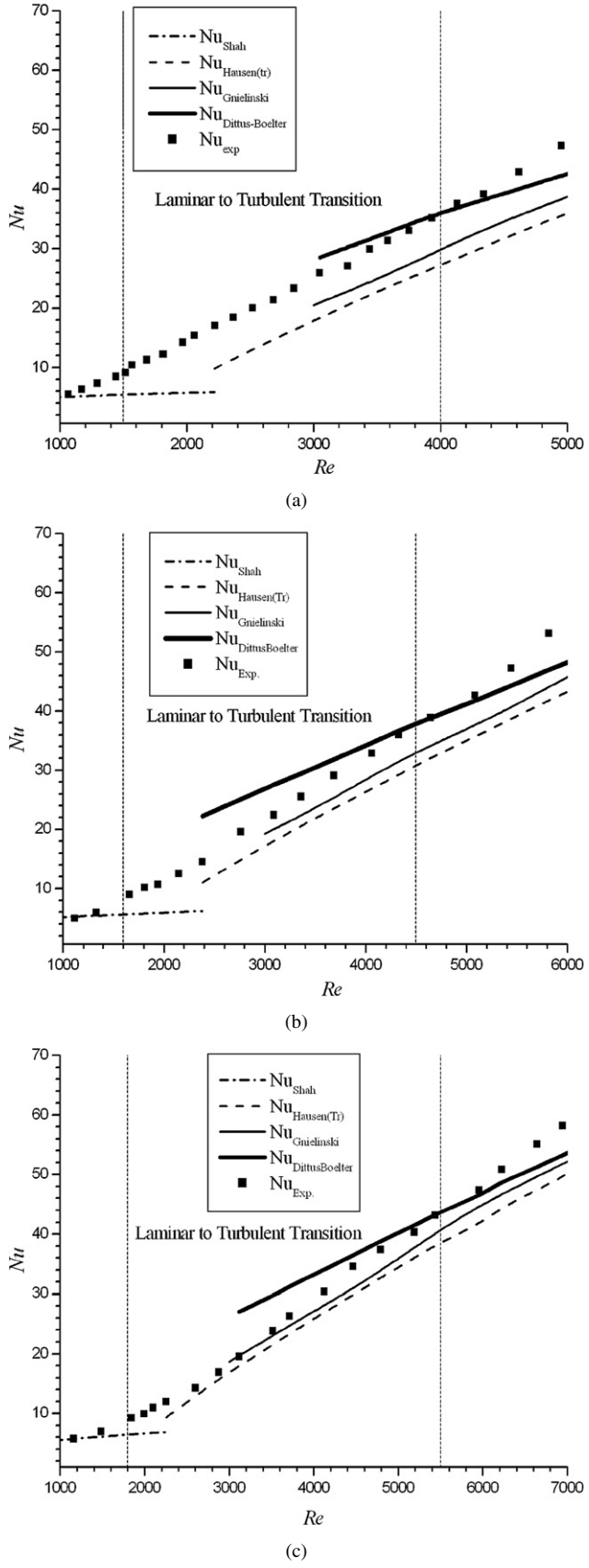

Fig. 7. Comparison of Nusselt numbers between experimental data and classical correlations ($1000 < Re < 7000$) for three microtubes at constant heat flux heating method: (a) $d = 242$ μm and $t_1 = 21.4\,^{\circ}\mathrm{C}$; (b) $d = 315$ μm and $t_1 = 21.8\,^{\circ}\mathrm{C}$; (c) $d = 520$ μm and $t_1 = 21.8\,^{\circ}\mathrm{C}$.

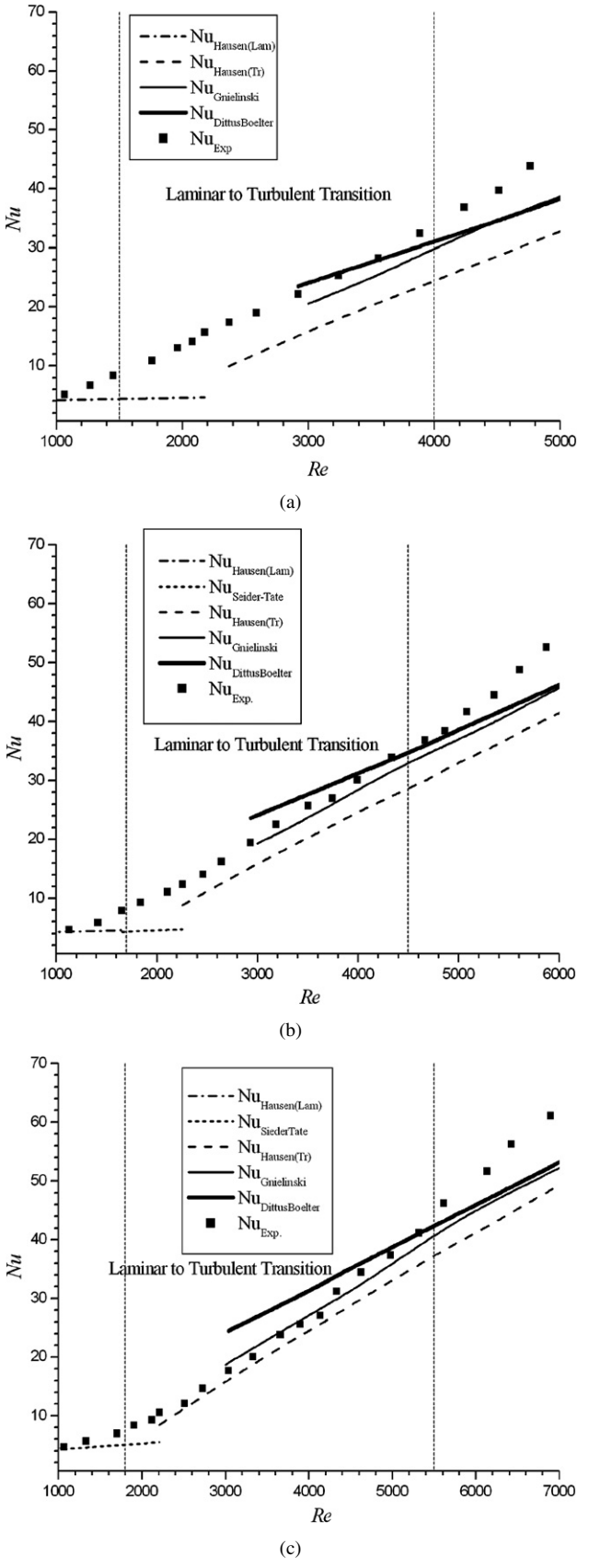

Fig. 8. Comparison of Nusselt numbers between experimental data and classical correlations ($1000 < Re < 7000$) for three microtubes at constant temperature heating method: (a) $d = 242$ μm and $t_1 = 22.6\,^{\circ}\mathrm{C}$; (b) $d = 315$ μm and $t_1 = 21.7\,^{\circ}\mathrm{C}$; (c) $d = 520$ μm and $t_1 = 23.4\,^{\circ}\mathrm{C}$.

Reynolds number reaches 4000, 4500 and 5500, respectively, for corresponding three type microtubes. So the laminar-to-turbulent transition region is indicated by two vertical dashed lines (Reynolds number varies from 1500 to 4000) according to the above analysis. Similarly, in Figs. 6 and 7, the transitional region appeared respectively at Reynolds number of 1600–4500 for microtube with the inner diameter of 315 μm and 1900–5500 for that of 520 μm.

The transitional region from laminar flow to turbulent flow is almost consistent for different heating methods though there are some deviations, shown in Figs. 7–8, which can be neglected considering the experimental uncertainties. However, even the Hausen correlation proposed for the transitional regime ($2200 < Re < 10000$) or the Gnielinski correlation for the transitional and the turbulent regime ($3000 < Re < 5 \times 10^6$) do not provide satisfactory predictions. It may be noted that entrance length effects are not accounted for in any of the turbulent flow correlations; even though entrance length effects are less important in turbulent flow, this may be a contributing factor to the observed discrepancies. In addition, there are not absolutely smooth in the microtubes, which can be seen from the SEM image of the cross-section of quartz glass microtubes, shown in Fig. 4. The wall roughness of the microtube can be up to 5–10 microns, and this may be other reason that causes the deviation of the experimental results from the classical correlations.

Though the experimental Nusselt numbers are larger than those predicted by the classical correlations, the experimental Nusselt numbers are closer to the heat transfer correlations with the increase of the inner diameters of microtube. For example, the experimental Nusselt numbers are very rough agreement with the correlations of Sieder–Tate and Hausen (laminar and transitional regime) for microtube with inner diameter of 520 μm, moreover, the slope of variation of the Nusselt number with the Reynolds number is approximately consistent with the predicted slopes from the Dittus–Boelter and the Gnielinski correlations. Additional results in the turbulent region are needed to address this question further, and to identify predictive correlations suitable to this regime and different mciroscale.

Comparisons of the experimental Nusselt number of two different heating methods are shown in Fig. 9.

The largest deviation for different heating methods can reach 30%, as indicated in Fig. 9(a), at lowest Reynolds number and the deviation decrease with the increase of the Reynolds number. Though there is always 15–20% deviation between the constant heating and the temperature heating at high Reynolds number, it is thought there is not any difference for two heating methods when Reynolds number is enough larger if the experimental uncertainties are considered.

Besides the experimental errors, the experimental Nusselt number at constant flux boundary condition should be larger than that at constant temperature boundary condition at laminar state, which has been demonstrated by the classical theory. The decrease of the deviation with the increase of the Reynolds number may be occurrence of the transitional flow.

From seen in Fig. 9, when Reynolds number exceeds a certain value, the differences will be less than 20% for two heating

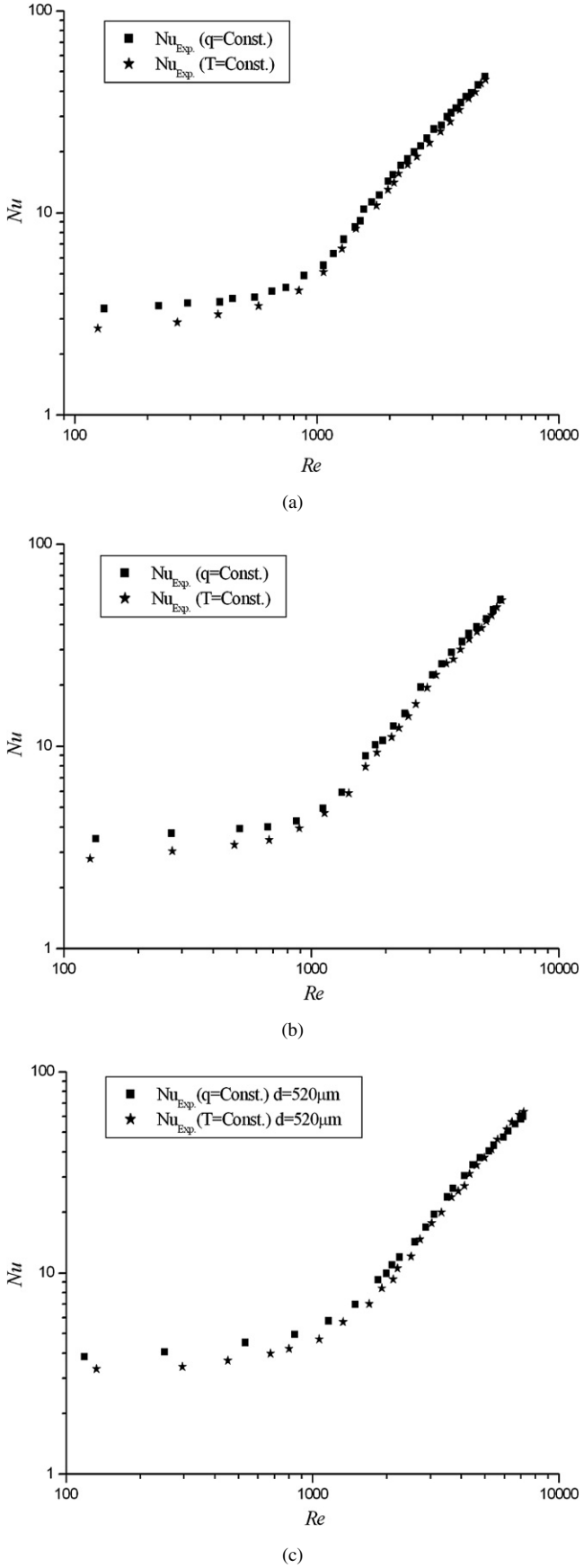

Fig. 9. Comparison Nusselt number between constant heat flux and constant temperature: (a) $d = 242$ μm; (b) $d = 315$ μm; (c) $d = 520$ μm.

methods. In this experiment, the critical values are 1200, 1900 and 2800, in accordance, for microtube with the inner diameter of 242 μm, 315 μm and 520 μm, respectively.

4. Conclusion

The forced convection heat transfer behaviors of deionized water flowing through microtubes with inner diameter of 242 μm, 315 μm and 520 μm were investigated experimentally. These microtubes were heated in two heating modes, approximately constant heat flux heating and constant temperature heating. Experimental tests were carried out in wide range of Reynolds numbers (100–7000), and the corresponding Nusselt numbers were obtained. Comparisons between the experimental results and those of the classical correlations lead to the following concluding remarks:

(1) The experimental Nusselt number is rough agreement with that of the laminar correlations when flow state is laminar unless Reynolds number is extremely low.
(2) The Reynolds numbers of the laminar-to-turbulent transition region may be about 1500–4000, 1600–4500 and 1900–5500 for microtubes with inner diameters of 242 μm, 315 μm and 520 μm, respectively;
(3) The influence of the heating method on the transitional region is small enough and may be neglected;
(4) The differences of the Nusselt numbers resulted from different heating methods can be neglected when Reynolds number is larger than 1200, 1900 and 2800 for microtubes with inner diameters of 242 μm, 315 μm and 520 μm, respectively.

Acknowledgements

The authors wish to acknowledge the financial support by the Academic frontier promotion program of the Japan Ministry of Education, Culture, Sports, Science and Technology and the Grant-in-aid for scientific research (C) from Japan Society for the Promotion of Science and the Academic frontier promotion program of mext Japan.

References

[1] D.R. Reyes, D. Iossifidis, P.A. Auroux, A. Manz, Micro total analysis system, introduction, theory and technology, Anal. Chem. 74 (12) (2002) 2623–2636.
[2] D.B. Tuckerman, R.F.W. Pease, High-performance heat sinking for VLSI, IEEE Electron. Dev. Lett. EDL 2 (1981) 126–129.
[3] G.H.M. Mala, D.Q. Li, Flow characteristics in microtubes, Int. J. Heat Fluid Flow 20 (1999) 142–148.
[4] T.M. Adams, S.I. Abdel-Khalik, S.M. Jeter, Z.H. Qureshi, An experimental investigation of single-phase forced convection in microchannels, Int. J. Heat Mass Transfer 41 (6–7) (1998) 851–857.
[5] D. Lelea, S. Nishio, K. Takano, The experimental research on microtube heat transfer and fluid flow of distilled water, Int. J. Heat Mass Transfer 47 (2004) 2817–2830.
[6] P.S. Lee, S.V. Garimella, D. Liu, Investigation of heat transfer in rectangular microchannels, Int. J. Heat Mass Transfer 48 (2005) 1688–1704.
[7] G.P. Celata, M. Cumo, M. Guglielmi, G. Zummo, Experimental investigation of hydraulic and single-phase heat transfer in 0.130 mm capillary tube, Microscale Thermophysical Engineering 6 (2002) 85–97.
[8] T.S. Ravigururajanm, J. Cuta, C.E. McDonald, M.K. Drost, Single-phase flow thermal performance characteristics of a parallel micro-channel heat exchanger, in: National Heat Transfer Conference, in: HTD, vol. 329 (7), ASME, 1996, pp. 157–166.
[9] Z.Y. Guo, Z.X. Li, Size effect on microscale single-phase flow and heat transfer, Int. J. Heat Mass Transfer 46 (2003) 149–159.
[10] G. Gamrat, M. Favre-Marinet, D. Asendrych, Conduction and entrance effects on laminar liquid flow and heat transfer in rectangular microchannels, Int. J. Heat Mass Transfer 48 (2005) 2943–2954.
[11] G. Maranzana, I. Perry, D. Maillet, Mini- and micro-channels: influence of axial conduction in the walls, Int. J. Heat Mass Transfer 47 (2004) 3993–4004.
[12] A.G. Fedorov, R. Viskanta, Three-dimensional Conjugate heat transfer in the microchannels heat sink for electronic packaging, Int. J. Heat Mass Transfer 43 (2000) 399–415.
[13] R.J. Moffat, Describing the uncertainties in experimental results, Exp. Thermal Fluid Sci. 1 (1988) 3–17.
[14] R.K. Shah, Thermal entry length solutions for circular tube and parallel plates, in: Proc. 3rd Natnal. Heat Mass Transfer Conference, Indian Inst. Technology Bombay 1, 1975, HTM-11-75.
[15] H. Hausen, Neue Gleichungen für die Wärmeübertragung bei freier und erzwungener Strömung, Allg. Wärmetchnik 9 (1959) 75–79.
[16] E.N. Sieder, G.E. Tate, Heat transfer and pressure drop of liquids in tubes, Industrial and Engineering Chemistry 28 (12) (1936) 1429–1435.
[17] S. Kakac, R.K. Shah, W. Aung, Handbook of Single-Phase Convective Heat Transfer, John Wiley and Sons, New York, 1987.
[18] V. Gnielinski, New equations for heat and mass transfer in turbulent pipe and channels flow, Int. Chem. Engrg. 16 (1976) 359–368.
[19] F.W.L. Dittus, M.K. Boelter, Heat transfer in automobile radiators of the tubular type, Univ. Calif. Publ. Engrg. 2 (13) (1930) 443–446.
[20] B.X. Wang, X.F. Peng, Experimental investigation on liquid forced convection heat transfer through microchannels, Int. J. Heat Mass Transfer 37 (1) (1994) 73–82.
[21] J. Li, G.P. Peterson, P. Cheng, Three-dimensional analysis of the heat transfer in a micro-heat sink with single phase flow, Int. J. Heat Mass Transfer 47 (2004) 4215–4231.